Int. J. Multiphase Flow Vol. 16, No. 2, pp. 305–321, 1990
Printed in Great Britain.

0301-9322/90 $3.00 + 0.00

LOW REYNOLDS NUMBER MOTION OF A DROPLET IN SHEAR FLOW INCLUDING WALL EFFECTS

M. SHAPIRA† and S. HABER
Technion—Israel Institute of Technology, Haifa 32000, Israel

(*Received* 20 *January* 1989; *in revised form* 10 *August* 1989)

Abstract—The hydrodynamic interaction between a droplet immersed in Couette flow and the containing walls is studied. The analysis is based on the assumptions that the disturbance flow induced by the droplet is without inertia, that the droplet maintains its nearly spherical shape and that the radius of the droplet is small compared with the distance between the walls. Based on Lorentz's reflection method, a first-order simple analytical solution is derived for the case of a droplet in close vicinity to one wall. An integral solution is given for the general configuration of a droplet interacting with two walls. First-order corrections for wall effects are obtained for the drag force and the droplet's deviation from sphericity.

Key Words: creeping flow, bubbles, droplets, wall effects

1. INTRODUCTION

The analysis of low Reynolds number flow around a single droplet moving between two infinite parallel flat plates is of fundamental importance in the field of lubrication. Lubricants are rarely free of contaminants and even a small amount of immersed bubbles would alter the performance of journal bearings and squeeze film dampers (see White 1970; Marsh 1974; Hibner & Bansal 1979; Parkins & Stanley 1982; Haber & Etsion 1985; Haber *et al.* 1987). In a typical journal bearing, the gap between the walls is very small, and interaction between the bubbles and the walls must be accounted for to avoid erroneous hydrodynamic predictions. The hydrodynamic interaction between adjacent bubbles seems, however, less significant and can be neglected.

The shape of immersed bubbles or droplets is not known *a priori* and is determined by the non-dimensional capillary number ($\mu Ga/\sigma$) where G is the local shear rate, μ is the viscosity of the lubricant, a is a characteristic dimension of the bubbles and σ is the surface tension. For small bubbles or weak shear rates, for which $\mu Ga/\sigma < 1$, the bubbles retain their nearly spherical shape (Taylor 1934; Bartok & Mason 1959; Chaffey & Brenner 1967; Cox 1969; Chan & Leal 1979). However, if $\mu Ga/\sigma$ is large the bubbles assume a needlelike shape or shatter to form smaller bubbles (Rumscheidt & Mason 1961a,b; Frankel & Acrivos 1970; Torza *et al.* 1972; Barthes-Biesel 1973; Acrivos & Lo 1978; Hinch & Acrivos 1980; Grace 1982). For small bubbles or droplets, a first-order approximation can be obtained if we assume that the bubbles are exactly spherical. This assumption makes it impossible to satisfy all the boundary conditions over the interface and, as shown by Hetsroni & Haber (1970), the condition for the normal component of the stress vector has to be abandoned. This condition, however, may in turn provide us with an estimate for the deviation of the droplet from sphericity.

The solution for the flow fields interior and exterior to a small spherical droplet moving in Couette flow can be viewed as a superposition of two simpler flow cases. The first case (1) is the flow field generated by a single droplet moving parallel to two infinite flat plates in a quiescent fluid. The second case (2) is the flow disturbance generated by an immobile droplet suspended in Couette flow. The second case can in turn be viewed as composed of two flow fields: (2a) a droplet suspended in a uniform field of magnitude G/h, where h is the distance of the center of the droplet from the immobile wall; and (2b) a droplet suspended in a "pure" shear field of zero velocity at the point occupied by the center of the droplet.

†Currently at California Institute of Technology, Pasadena, CA 91125, U.S.A.

Case 2a is identical, from the mathematical point of view, to case 1. Consequently, the general problem of a droplet or bubble moving in Couette flow can be divided into two subproblems: the aforementioned cases 1 and 2b. The first case was analyzed in a previous paper (Shapira & Haber 1988). Analysis of case 2b is the goal of the present work.

The paper is divided into three main parts. In the first part (section 4), we briefly present the results for a droplet suspended in pure shear flow close to a *single* flat wall. This case is associated with the geometrical configuration of a small bubble ($a/h < 1$) suspended close to one wall ($h/H \ll 1/2$), where H is the gap between the walls. In the second part (section 5), we consider the geometrical configuration of a bubble suspended between two walls, namely, $h/H \approx 1/2$ and compare it with the results obtained by Chan & Leal (1979). In the third part (section 6), a comparison between the two configurations is made so that one can deduce the values of h/H for which a single wall effect analysis is sufficient.

2. STATEMENT OF THE PROBLEM

A small spherical droplet of radius a is suspended between two flat parallel walls, a distance H apart. The center of the droplet is at a distance h from one of the walls (denoted henceforth as wall 1). The flow field far from the droplet is $\mathbf{v}_\infty = G(z-h)\mathbf{i}$, where G is the shear rate, (x, y, z) form a cartesian coordinate system which is located at the projection point of the droplet center onto wall 1 and $(\mathbf{i}, \mathbf{j}, \mathbf{k})$ is the associated orthonormal set of unit vectors.

The fluids interior and exterior to the droplet are homogeneous, isothermal, Newtonian and of constant density, and the Reynolds number Ga^2/ν is sufficiently small for Stokesian flow to be assumed.

For the continuous phase, the field equations are

$$\nabla^2\mathbf{u} = \frac{1}{\mu}\nabla p, \qquad \nabla\cdot\mathbf{u} = 0. \tag{1}$$

Similarly, for the dispersed phase, we have

$$\nabla^2\mathbf{u}' = \frac{1}{\mu'}\nabla p', \qquad \nabla\cdot\mathbf{u}' = 0; \tag{2}$$

where $\mathbf{u}$ and p stand for the velocity and pressure fields, respectively, and μ is the viscosity. The primed symbols refer to variables inside the droplet.

The no slip boundary conditions over the walls are

$$\mathbf{u} = -Ghi \qquad @\ z = 0, H \tag{3}$$

and over the surface of the droplet δS it implies that

$$\mathbf{u} = \mathbf{u}' \qquad @\ \delta S. \tag{4}$$

No mass transfer through the interface results in

$$\mathbf{u}\cdot\mathbf{i}_n = 0 \qquad @\ \delta S, \tag{5}$$

where $\mathbf{i}_n$ is a unit vector normal to δS.

The condition of continuous shear stress and the jump condition for the normal component of the stress vector $\boldsymbol{\pi} \equiv \underline{\boldsymbol{\pi}}\cdot\mathbf{i}_n$ (due to surface tension) can be written as

$$\pi_n - \pi_n' = \sigma\left(\frac{1}{R_1}+\frac{1}{R_2}\right)\mathbf{i}_n \qquad @\ \delta S, \tag{6}$$

where $\underline{\boldsymbol{\pi}}$ is the stress tensor, σ is the surface tension and R_1 and R_2 are the principal radii of the surface.

Only the two tangential components of [6] would be utilized to determine the velocity fields for a slightly deformed droplet. The normal component would be used to estimate the deviation of the droplet shape from sphericity (see Hetsroni & Haber 1970).

3. THE GENERAL METHOD OF SOLUTION

The solution is based on the method of reflection that is described by Happel & Brenner (1965) and modified by Shapira & Haber (1988) to enhance numerical convergence. According to the traditional reflection method, boundary conditions at the wall and at the droplet interface are satisfied alternately. An odd numbered reflection rectifies the error over the droplet interface that is induced by the previous even numbered reflection (assuming no walls exist in the space occupied by the fluid). An even numbered reflection rectifies the error at the wall that was induced by a previous odd reflection (assuming no droplet exists in the space occupied by the fluid).

According to the modified reflection scheme, an odd reflection employs a set of boundary conditions which includes those over the droplet interface *and* the two tangential velocity components over the wall. An even reflection rectifies the error in the boundary condition over the wall associated with the normal velocity component only.

A major advantage of the modified scheme can be explained as follows. The disturbance induced by a droplet moving in an unbounded field dies out like $1/r$ for large distances r from the droplet. However, if one examines the asymptotic behavior of the velocity components far downstream (or upstream) and at a finite small radial distance from the motion axis, one reveals that the velocity components parallel to this axis die out like $1/r$, whereas the velocity components perpendicular to it die out like $1/r^2$. Consequently, satisfying simultaneously the boundary conditions for the tangential velocity components over the wall and the boundary conditions over the droplet interface eliminates a very slow converging mode from the reflection procedure, whereas the faster converging mode, the one associated with the normal velocity component at the wall, is taken care of by successive reflections. It is therefore believed that this modified scheme causes the numerical integration to converge more rapidly than the simple method. In essence, three reflections would be sufficient to capture the main characteristics of the flow field. However, if the main interest lies in obtaining the drag force exerted on the droplet, the generalized Faxen law for droplets (Hetsroni & Haber 1970) can be applied and two reflections would suffice to derive a third reflection order of accuracy. Thus, the velocity and pressure fields external to the droplet can be expressed as the sum of three fields:

$$\mathbf{u} = \mathbf{v}_\infty + \mathbf{v} + \boldsymbol{\omega}; \qquad p = p_\infty + q + s, \qquad [7]$$

where $\mathbf{v}_\infty = G(z-h)\mathbf{i}$ is the undisturbed velocity field, $\mathbf{v}$ and $\boldsymbol{\omega}$ are the first and second velocity reflections, respectively, and q and s are the respective pressure fields.

All three fields satisfy the field equation [1] separately. The solution domain of the first reflection $\mathbf{v}$ is the space bounded by the walls and the droplet interface, whereas the solution domain of the second reflection $\boldsymbol{\omega}$ is bounded by the walls only.

The boundary conditions satisfied by the first reflection $\mathbf{v}$ are: (a) the boundary conditions over the droplet interface [4]–[6] ($\mathbf{u}$ must be replaced by $\mathbf{v}+\mathbf{v}_\infty$ and the stress tensor $\underline{\boldsymbol{\pi}}$ is based on $\mathbf{v}+\mathbf{v}_\infty$); (b) the no slip boundary conditions at the wall for the tangential components,

$$\mathbf{v}\cdot\mathbf{i} = \mathbf{v}\cdot\mathbf{j} = 0 \qquad @\ z = 0, H; \qquad [8, 9]$$

and (c) the disturbance dies out at infinity,

$$\mathbf{v} \to 0 \qquad @\ x, y, z \to \infty. \qquad [10]$$

(Tacitly we assumed that for the $\mathbf{v}\cdot\mathbf{k}$ component the wall does not exist and [9] is required for the entire domain external to the droplet.) The boundary conditions satisfied by the second reflection nullify the velocity component normal to the walls which was induced by $\mathbf{v}$, namely:

$$\boldsymbol{\omega} = -\mathbf{v} \qquad @\ z = 0, H. \qquad [11]$$

It can easily be verified that the velocity sum [7] satisfies exactly the boundary conditions over the walls, whereas the boundary conditions over the droplet interface are only approximately satisfied due to the small velocity induced by $\boldsymbol{\omega}$.

4. DROPLET CLOSE TO A SINGLE WALL

4.1. The flow field

We briefly present the solution for a droplet placed in close vicinity to a single wall so that $h/H \ll 1$. Chaffey *et al.* (1965); Chaffey & Brenner (1967), who addressed a similar problem, investigated the effect of a droplet settling perpendicular to the streamlines due to droplet deformation. We, however, investigate the wall effects on the settling velocity parallel to the streamlines and on droplet deformation.

The semi-infinite domain of the first reflection can be replaced by an equivalent infinite domain which contains two droplets, the second droplet being a mirror image of the original droplet.

The first reflection $\mathbf{v}$ constitutes the disturbance introduced by the droplets. It can be described as a superposition of the flow $\mathbf{v}_1$ and $\mathbf{v}_2$:

$$\mathbf{v} = \mathbf{v}_1 + \mathbf{v}_2, \tag{12}$$

where

$$\mathbf{v}_1 = \left\{-\mathrm{A}\frac{(z-h)x^2}{r_1^5} - \mathrm{B}\left[\frac{(z-h)}{r_1^5} - 5\frac{(z-h)x^2}{r_1^7}\right]\right\}\mathbf{i} + \left[-\mathrm{A}\frac{(z-h)xy}{r_1^5} + 5\mathrm{B}\frac{(z-h)xy}{r_1^7}\right]\mathbf{j} + \left\{-\mathrm{A}\frac{(z-h)^2x}{r_1^5} - \mathrm{B}\left[\frac{x}{r_1^5} - 5\frac{(z-h)^2x}{r_1^7}\right]\right\}\mathbf{k} \tag{13}$$

is the flow disturbance generated by the first droplet located at $z = h$ and suspended in an unbounded shear flow $\mathbf{v}_\infty = G(z-h)\mathbf{i}$ and

$$\mathbf{v}_2 = \left\{-\mathrm{A}\frac{(z+h)x^2}{r_2^5} - \mathrm{B}\left[\frac{(z+h)}{r_2^5} - 5\frac{(z+h)x^2}{r_2^7}\right]\right\}\mathbf{i} + \left[-\mathrm{A}\frac{(z+h)xy}{r_2^5} + 5\mathrm{B}\frac{(z+h)xy}{r_2^7}\right]\mathbf{j} + \left\{-\mathrm{A}\frac{(z+h)^2x}{r_2^5} - \mathrm{B}\left[\frac{x}{r_2^5} - 5\frac{(z+h)^2x}{r_2^7}\right]\right\}\mathbf{k} \tag{14}$$

is the flow disturbance generated by the second droplet located at $z = -h$ and suspended in an unbounded shear flow $\mathbf{v}_\infty = G(z+h)\mathbf{i}$. Here r_1 and r_2 are the radial from the center of the first and the second droplet, respectively,

$$r_1 = [(z-h)^2 + x^2 + y^2]^{1/2} \tag{15a}$$

and

$$r_2 = [(z+h)^2 + x^2 + y^2]^{1/2}, \tag{15b}$$

and A and B are constants,

$$\mathrm{A} = \frac{\mu + 2.5\mu'}{\mu + \mu'} Ga^3 \tag{16}$$

and

$$\mathrm{B} = \frac{\mu'}{2(\mu + \mu')} Ga^5. \tag{17}$$

The pressure fields generated by a droplet at $z = h$ and a second droplet at $z = -h$ are, respectively,

$$q_1 = -2\mu A\frac{(z-h)x}{r_1^5} \tag{18}$$

and

$$q_2 = -2\mu A\frac{(z+h)x}{r_2^5}. \tag{19}$$

Their total

$$q = q_1 + q_2 \qquad [20]$$

forms the contribution to the pressure field of the first reflection. It is clearly indicated that over the wall ($z = 0$), we have that $r_1 = r_2$ and q is zero as expected.

The disturbance field of the second reflection ω stems from the non-zero velocity component normal to the wall that is generated by the first reflection.

$$v_z = \mathbf{v} \cdot \mathbf{k} = (\mathbf{v}_1 + \mathbf{v}_2) \cdot \mathbf{k} = -\frac{2Ah^2x}{(h^2 + \rho^2)^{5/2}} \qquad @\ z = 0, \qquad [21]$$

where

$$\rho^2 = x^2 + y^2. \qquad [22]$$

Thus a flow field ω is sought in the semi-infinite domain $z > 0$, for which

$$\left.\begin{aligned} \omega \cdot \mathbf{k} &= \frac{2Ah^2x}{(h^2 + \rho^2)^{5/2}} \\ \omega \cdot \mathbf{i} &= 0 \\ \omega \cdot \mathbf{i} &= 0 \end{aligned}\right\} \quad @\ z = 0. \qquad [23a\text{–}c]$$

Utilizing a two-dimensional Fourier integral transform and Lipshitz equality (see appendix A), one obtains an extremely simple analytical solution for ω, namely,

$$\omega = \frac{2Ah}{r_2^7}\{\mathbf{i}z(h + z)(5x^2 - r_2^2) + \mathbf{j} \cdot 5z(h + z)xy + \mathbf{k}x[hr_2^2 + 5z(h + z)^2]\}, \qquad [24]$$

where r_2 is given by [14]. The associated pressure field is

$$s = \frac{4Ah\mu x}{r_2^7}[5(h + z)^2 - r_2^2], \qquad [25]$$

which is antisymmetric with respect to the $x = 0$ plane and symmetric with respect to the $y = 0$ plane, as expected.

4.2. The drag force

The third reflection would correct the boundary conditions over the droplet interface (violating the boundary conditions over the wall only slightly). The correction to be made stems from the disturbance generated by the image droplet and the velocity induced by the second reflection. The exact velocity distribution is of no particular interest, since the resultant drag force and the change in the droplet shape can be obtained using the generalized Faxen law (Hetsroni & Haber 1970):

$$\mathbf{F}_D = 6\pi\mu a \frac{\frac{2}{3}\mu + \mu'}{\mu + \mu'}[\mathbf{V}_\infty]_{r=0} + \pi a^3 \frac{\mu'}{\mu + \mu'}[\nabla^2 \mathbf{V}_\infty]_{r=0}, \qquad [26]$$

where in our case $[\mathbf{V}_\infty]$, the undisturbed velocity field, is

$$\mathbf{V}_\infty = \mathbf{v}_\infty + \mathbf{v}_2 + \omega \qquad [27]$$

and the location $r = 0$ in [26] refers to the origin of the droplet, namely, $x = y = 0$ and $z = h$.

The second term in [26] is of a higher order than $(a/h)^2$ and therefore would be neglected. Introducing [24] into [26], we obtain

$$\mathbf{F}_D = -\mathbf{i}\tfrac{1}{2}\pi\mu G a^2 \frac{(\frac{3}{2}\mu' + \mu)(\frac{5}{2}\mu' + \mu)}{(\mu' + \mu)^2}\left(\frac{a}{h}\right)^2 + O\left(\frac{a}{h}\right)^4, \qquad [28]$$

where the contribution of $\mathbf{v}_\infty$ is identically zero and that of $\mathbf{v}_2$ was found to be of order $(a/h)^4$.

The total wall effect on the drag force is provided by [28] since for a droplet submerged in an unbounded shear flow the net drag force is zero. Equation [28] also proves that the only non-vanishing force component (for a spherical droplet) is parallel to the wall so that no droplet migration perpendicular to the wall is expected (as long as the droplet remains spherical). The

negative sign in [28] proves that a small droplet would lag behind the undisturbed Couette flow if located close to the immobile wall. This is in agreement with the known wall effect for a particle moving close to the wall inside Poiseuille flow (Happel & Brenner 1965).

The net perpendicular force exerted on the wall is zero since the net contribution of $q_1 + q_2$ over the wall vanishes and s is antisymmetric with respect to the $x = 0$ plane. Integration of the pressure field over the conduit walls reveals that no net torque is exerted on the walls due to the presence of the droplet It stems from the sign change that the pressure field [25] undergoes across the circle $x^2 + y^2 = 4h^2$.

4.3. Droplet deformation

If r, θ, φ is a spherical coordinate system located at the droplet origin, the deformed shape of the droplet can be expressed by

$$r = a[1 + \delta(\theta, \varphi)], \qquad [29]$$

where a first-order term can be derived from the following relation:

$$\delta(\theta, \varphi) = \frac{\mu a}{\sigma} \frac{16\mu + 19\mu'}{8(\mu + \mu')} \left[\frac{\partial V_{r\infty}}{\partial r}\right]_{r=0}; \qquad [30]$$

following Hetsroni & Haber (1970) and Shapira & Haber (1988). Here $V_{r\infty}$ is the radial component of $\mathbf{V}_\infty$ given in [27]. The first term in [27], $\mathbf{v}_\infty$ (no wall effects), contributes to the deformation observed by Taylor (1934):

$$\delta_T = \frac{\mu G a}{\sigma} \frac{16\mu + 19\mu'}{8(\mu + \mu')} \sin\theta \cos\theta \cos\phi, \qquad [31]$$

where θ is the latitude angle measured from the z axis and ϕ is the azimuthal angle measured from the x axis. Substituting the last two terms of [27] into [30], we obtain

$$\delta_W = \frac{3}{8}\left(\frac{a}{h}\right)^3 \cdot \frac{\mu G a}{\sigma} \cdot \frac{16\mu + 19\mu'}{8(\mu + \mu')} \cdot \frac{\mu + 2.5\mu'}{\mu + \mu'} \cdot \sin\theta \cos\theta \cos\phi, \qquad [32]$$

which is solely due to wall effects, and the total deformation is

$$\delta = \delta_T + \delta_W. \qquad [33]$$

Thus, a droplet in close vicinity to the wall has a larger deformation but no change in shape, an ellipsoid tilted along the flow direction and inclined 45° from the wall.

5. A DROPLET BETWEEN TWO PARALLEL WALLS

The problem addressed in section 2 dealt with the case of a droplet close to a single wall so that $h/H \ll 1$. However, if the latter condition is not satisfied, the effect of both walls must be accounted for.

The method of solution for a droplet interacting with two walls is somewhat similar to the previous problem. For the first reflection, we would try again to satisfy the boundary conditions pertaining to the tangential velocity components over the walls and over the droplet interface. The second reflection would rectify the solution so that the velocity component perpendicular to the walls would vanish. Finally, the third reflection contribution would be accounted for insofar as the drag force and the deformation of the droplet are concerned.

5.1. The solution

An exact solution, for which we satisfy simultaneously the boundary conditions for the tangential velocity components over the wall and over the droplet interface, is formidable. Indeed, it is redundant, since the solution scheme is carried out up until the second reflection which, in turn, satisfies only approximately the boundary conditions over the droplet interface. Hence, an approximate first reflection, consistent with the order of accuracy of the second reflection is sufficient. Here we utilize again the previous technique to extend the flow domain to infinity. This time an infinite number of mirror images of the droplet and the non-disturbed velocity field are

required so that the tangential velocity components vanish simultaneously over both walls (see Shapira & Haber 1988). An approximate flow field for the disturbance velocity due to this periodic configuration is the sum

$$\mathbf{v} = \mathbf{v}_1 + \mathbf{v}_2 = \sum_{m=-\infty}^{\infty} \{\mathbf{v}_1^m + \mathbf{v}_2^m\}, \qquad [34]$$

where $\mathbf{v}_1^m$ and $\mathbf{v}_2^m$ possess the form of [12] and [13], respectively; only h must be replaced by $h + 2mH$, the z location of the image droplets. It is easy to show by direct substitution that at $z = 0$ and $z = H$ the tangential components vanish. The boundary conditions over the droplet interface are only approximately satisfied and the error induced by the image droplets and the second reflection could be corrected by a third reflection velocity field. The non-vanishing velocity component perpendicular to the wall at $z = 0$ is

$$v_z = -2Ax \sum_{m=-\infty}^{\infty} \frac{(h + 2mH)^2}{r_m^5} \qquad @\ z = 0, \qquad [35]$$

where

$$r_m^2 = (h + 2mH^2) + x^2 + y^2; \qquad [36]$$

and at $z = H$, we have

$$v_z = -2Ax \sum_{m=-\infty}^{\infty} \frac{[h + (2m + 1)H]^2}{R_m^5}, \qquad [37]$$

where

$$R_m^2 = [h + (2m + 1)H]^2 + x^2 + y^2. \qquad [38]$$

Here again we neglected the terms perceded by the B coefficient which are of higher order in a/h. Similar to the previous problem, the pressure field induced by $\mathbf{v}$ over the walls is identically zero.

To nullify the velocity components normal to the walls, the second reflection must satisfy the following boundary conditions:

$$\omega_z = 2Ax \sum_{m=-\infty}^{\infty} \frac{(h + 2mH)^2}{r_m^5} \qquad @\ z = 0, \qquad [39a]$$

$$\omega_z = 2Ax \sum_{m=-\infty}^{\infty} \frac{[h + (2m + 1)H]^2}{R_m^5} \qquad @\ z = H \qquad [39b]$$

and

$$\omega_x = \omega_y = 0 \qquad @\ z = 0, H. \qquad [39c]$$

The general solution in cartesian coordinates is again utilized (see appendix A). This time, however, we must keep the full expression [A.4]. Equations [39a–c] suggest that the following modified form of [A.4] would result in simpler algebraic equations for the unknown coefficients, namely, for the transformed velocity components we use the expressions,

$$\tilde{\omega}_x = \left[\tilde{E} - \frac{i\lambda_1}{\lambda}(z - H)\tilde{D}\right]\cosh \lambda z + \left[\tilde{F} - \frac{i\lambda_1}{\lambda}(z - H)\tilde{C}\right]\sinh \lambda z, \qquad [40a]$$

$$\tilde{\omega}_y = \left[\tilde{I} - \frac{i\lambda_2}{\lambda}(z - H)\tilde{D}\right]\cosh \lambda z + \left[\tilde{J} - \frac{i\lambda_2}{\lambda}(z - H)\tilde{C}\right]\sinh \lambda z \qquad [40b]$$

and

$$\tilde{\omega}_z = [\tilde{A} + (z - H)\tilde{C}]\cosh \lambda z + [\tilde{B} + (z - H)\tilde{D}]\sinh \lambda z, \qquad [40c]$$

and for the transformed pressure we use

$$\tilde{s} = 2(\tilde{E} \cosh \lambda z + \tilde{D} \sinh \lambda z), \qquad [41]$$

where $\tilde{A}$ to $\tilde{J}$ are eight, as yet unknown, coefficients (functions of λ_1 and λ_2 in general). To satisfy the continuity equation it is required that

$$\tilde{C} = i(\lambda_1 \tilde{E} + \lambda_2 \tilde{I}) - \lambda \tilde{B} \tag{42a}$$

and

$$\tilde{D} = i(\lambda_1 \tilde{F} + \lambda_2 \tilde{J}) - \lambda \tilde{A}, \tag{42b}$$

limiting the number of unknown independent coefficients to six, the exact number of scalar boundary conditions over the walls. Introducing [39c] into [40a–c], we obtain the following relations for $\tilde{C}$ to $\tilde{J}$ in terms of $\tilde{A}$ and $\tilde{B}$:

$$\tilde{C} = -\frac{\lambda \tilde{A} \beta}{(1 + \beta \coth \beta)} - \lambda \tilde{B}, \quad \tilde{D} = -\frac{\lambda \tilde{A}}{(1 + \beta \coth \beta)}, \quad \tilde{E} = \frac{i\beta_1 \tilde{A}}{(1 + \beta \coth \beta)},$$
$$\tilde{F} = -\frac{i\beta_1 \coth \beta \tilde{A}}{(1 + \beta \coth \beta)}, \quad \tilde{I} = \frac{i\beta_2 \tilde{A}}{(1 + \beta \coth \beta)} \quad \text{and} \quad \tilde{J} = -\frac{i\beta_2 \coth \beta \tilde{A}}{(1 + \beta \coth \beta)}, \tag{43}$$

where β, β_1 and β_2 are the following dimensionless parameters:

$$\beta = \lambda H, \quad \beta_1 = \lambda_1 H, \quad \beta_2 = \lambda_2 H. \tag{44}$$

Utilizing the identities (see appendix B)

$$\sum_{m=-\infty}^{\infty} \frac{2Ax(h + 2mH)^2}{r_m^5} = -\frac{A}{3\pi} \int\int_{-\infty}^{\infty} i\lambda_1 \frac{\partial}{\partial \lambda} \left(\frac{\cosh \lambda (H - h)}{\sinh \lambda H} \right) \exp[-i(\lambda_1 x + \lambda_2 y)] \, dx \, dy \tag{45a}$$

and

$$\sum_{m=-\infty}^{\infty} \frac{2Ax[h + (2m + 1)H]^2}{R_m^5} = -\frac{A}{3\pi} \int\int_{-\infty}^{\infty} i\lambda_1 \frac{\partial}{\partial \lambda} \left(\frac{\cosh \lambda h}{\sinh \lambda H} \right) \exp[-i(\lambda_1 x + \lambda_2 y)] \, dx \, dy \tag{45b}$$

and [39a, b] make it possible to derive $\tilde{A}$ and $\tilde{B}$ in terms of k and t:

$$\frac{\tilde{A}}{\frac{iA\beta_1}{3\pi}} \equiv \tilde{a} = \frac{(k \sinh \beta - t\beta)(\sinh \beta + \beta \cosh \beta)}{\sinh^2 \beta - \beta^2} \tag{46}$$

and

$$\frac{\tilde{B}}{\frac{iA\beta_1}{3\pi}} \equiv \tilde{b} = \frac{t\beta^2 \sinh \beta - (k \cosh \beta - t)(\sinh \beta + \beta \cosh \beta)}{\sinh^2 \beta - \beta^2}, \tag{47}$$

where

$$k = -\frac{\partial}{\partial \beta} \left(\frac{\cosh(1 - \hat{h})\beta}{\sinh \beta} \right), \tag{48a}$$

$$t = -\frac{\partial}{\partial \beta} \left(\frac{\cosh \hat{h}\beta}{\sinh \beta} \right) \tag{48b}$$

and

$$\hat{h} = \frac{h}{H}. \tag{49}$$

Introducing [43] and [44] into [40] and utilizing the fact that the two-dimensional Fourier transform is equal to the zero-order Hankel transform, we obtain for the velocity components parallel to the walls

$$\omega_x = -\frac{2}{3} \frac{A}{H^2} \frac{\partial^2}{\partial \hat{x}^2} \int_0^{\infty} \beta J_0(\hat{\rho}\beta) \left\{ \frac{\tilde{a}}{(1 + \beta \coth \beta)} [-\hat{z} \cosh(\hat{z}\beta) + \coth \beta \sinh(\hat{z}\beta) \right.$$
$$\left. + \beta(1 - \hat{z}) \sinh(\hat{z}\beta)] + \tilde{b}(1 - \hat{z}) \sinh \hat{z}\beta \right\} d\beta \tag{50}$$

and

$$\omega_y = -\frac{2}{3}\frac{A}{H^2}\frac{\partial^2}{\partial\hat{x}\,\partial\hat{y}}\int_0^\infty \beta J_0(\hat{\rho}\beta)\{\quad\}\,d\beta, \qquad [51]$$

where the expressions in curly brackets in [51] and [50] are identical and

$$\hat{x} = \frac{x}{H}, \quad \hat{y} = \frac{y}{H}, \quad \hat{z} = \frac{z}{H} \quad \text{and} \quad \hat{\rho} = \frac{\rho}{H} = \frac{(x^2+y^2)^{1/2}}{H}$$

are dimensionless coordinates.

The velocity component perpendicular to the wall is

$$\omega_z = -\frac{2}{3}\frac{A}{H^2}\frac{\partial}{\partial\hat{x}}\int_0^\infty \beta J_0(\hat{\rho}\beta)\left\{\frac{\tilde{a}}{1+\beta\coth\beta}[\cosh(\hat{z}\beta)(1+\beta\coth\beta)+\beta^2(1-\hat{z})\cosh\hat{z}\beta + \beta(1-\hat{z})\sinh\hat{z}\beta] + \tilde{b}[\sinh\hat{z}\beta+\beta(1-\hat{z})\cosh\hat{z}\beta]\right\}d\beta. \qquad [52]$$

If numerical integration of [50]–[52] is desired, one can differentiate with respect to $\tilde{x}$ and $\tilde{y}$ prior to integrating the equation, since the only term in the integrands depending on $\tilde{x}$ and $\tilde{y}$ is the zero-order Bessel function $J_0(\hat{\rho}\beta)$.

The pressure disturbance s due to the velocity field ω is obtained using [41], [43] and [44]:

$$s = \mu\frac{4}{3}\frac{A}{H^3}\frac{\partial}{\partial\hat{x}}\int_0^\infty \beta J_0(\hat{\rho}\beta)\left\{\left[\frac{\tilde{a}\beta^2}{(1+\beta\coth\beta)}+\tilde{b}\beta\right]\cosh(\hat{z}\beta)+\frac{\tilde{a}\beta}{1+\beta\coth\beta}\sinh\hat{z}\beta\right\}d\beta$$

$$= -\frac{4}{3}\frac{A\mu}{H^3}\frac{\hat{x}}{\hat{\rho}}\int_0^\infty \beta^2 J_1(\hat{\rho}\beta)\left\{\frac{\tilde{a}(\beta^2\cosh\hat{z}\beta+\beta\sinh\hat{z}\beta)}{(1+\beta\coth\beta)}+\tilde{b}\beta\cosh\hat{z}\beta\right\}d\beta \qquad [53]$$

5.2. The drag force

The contribution to the drag force of reflections lower than three is identically zero. Keeping terms of order $(a/H)^2$ only, the contribution of the third reflection can be derived by using the generalized Faxen law, namely [50]–[52] are introduced into [26] and evaluated at $x = y = 0$ and $z = h$. One can easily show that only the first term of [26] contributes to the desired accuracy and that no net drag force exists in the y and the z directions. In other words, no lift or side forces are exerted on the droplet. However, in the x direction, the direction of the undisturbed shear flow, we obtain that

$$\mathbf{F}_D = 4\pi\mu G a^2\frac{(\mu+\frac{3}{2}\mu')(\mu+\frac{5}{2}\mu')}{(\mu+\mu')^2}\left(\frac{a}{H}\right)^2 C_D\mathbf{i}, \qquad [54a]$$

where the drag force coefficient is

$$C_D = \frac{1}{3}\int_0^\infty \frac{\beta^3}{\sinh^2\beta-\beta^2}\{(1-\hat{h})\sinh\hat{h}\beta(t\sinh\beta-k\beta)+\hat{h}\sinh(1-\hat{h})\beta(t\beta-k\sinh\beta)\}\,d\beta \qquad [54b]$$

where k and t are given in [48a,b].

Convergence of [54b] is assured since the integrand of [54b] tends to zero for $\beta\to 0$ as $3\hat{h}(1-\hat{h})(1-2\hat{h})\beta$ and for large β and $\hat{h} < \frac{1}{2}$ it decays exponentially as $-\hat{h}^2\beta^3\exp(-2\hat{h}\beta)$. For $\hat{h} = \frac{1}{2}$, C_D is exactly zero, as required by symmetry, and for $\hat{h}$ and $1-\hat{h}$ the results are equal in magnitude and opposite in sign. Figure 1 depicts C_D as a function of $\hat{h} = h/H$ for droplets not too close to the walls. It manifests obviously that wall effects become more significant as the droplet moves closer to the wall. The asymptotic behavior of C_D for small values of $\hat{h}$ is (see appendix C),

$$\lim_{\hat{h}\to 0} C_D\cdot\hat{h}^2 = -\tfrac{1}{8}, \qquad [55]$$

which coincides with the result given in [28]. Consequently, for the above case the drag force coefficient grows at a faster rate than that of a particle moving in quiescent fluid in which C_D grows like $1/\hat{h}$. The contribution [54a,b] to the drag force is wholly due to wall effects, since for an unbounded shear flow the drag force is identically zero.

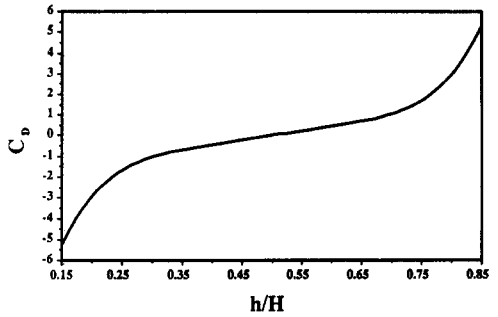

Figure 1. Drag force coefficient [54b] vs droplet position.

5.3. Droplet deformation

Following the analysis of section 2.5, the total deformation of a droplet is due to two contributions: the unbounded contribution [31] due to Taylor and the wall effect due to **v** and ω. Only that part of **v** which is induced by the mirror images of the droplet must be considered. Thereby, the contribution of $\mathbf{v}_1^0$ in [34], which represents the flow induced by the original droplet, must not be accounted for. The radial velocity component of $\mathbf{v}_1$ [cf. 34] we use in [30] is

$$v_{1r} = \frac{1}{r}[xv_{1x} + yv_{1y} + (z-h)v_{1z}] = -\sum_{\substack{m=-\infty \\ m\neq 0}}^{\infty} \frac{Ax}{rr_m^5}[z-(h+2mH)] \times \{x^2 + y^2 + (z-h)[z-(h+2mH)]\}. \quad [56]$$

Equation [56] can be rewritten using a spherical coordinate system

$$v_{1r} = -\sum_{\substack{m=-\infty \\ m\neq 0}}^{\infty} \frac{Ar\sin\theta}{r_m^5}\cos\phi(r\cos\theta - 2mH)[r\sin^2\theta + \cos\theta(r\cos\theta - 2mH)], \quad [57]$$

where (r, θ, φ) is a spherical coordinate system located at the center of the droplet. Thus,

$$\left.\frac{\partial v_{1r}}{\partial r}\right|_{r=0} = -\frac{1}{4}\frac{A}{H^3}\sin\theta\cos\theta\cos\phi\sum_{m=1}^{\infty}\frac{1}{m^3}. \quad [58]$$

Similarly, the contribution of $\mathbf{v}_2$ is

$$\left.\frac{\partial v_{2r}}{\partial r}\right|_{r=0} = -\frac{A}{8H^3}\sin\theta\cos\theta\cos\phi\left[\sum_{m=0}^{\infty}\frac{1}{(m+\hat{h})^3} + \sum_{m=1}^{\infty}\frac{1}{(m-\hat{h})^3}\right]. \quad [59]$$

The radial velocity component of ω is

$$\omega_r = \frac{1}{r}[x\omega_x + y\omega_y + (z-h)\omega_z]. \quad [60]$$

Introducing [50]–[52] into [60], we obtain

$$\omega_r = -\frac{2}{3}\frac{A}{H^2}\sin\theta\cos\phi\left(\int_0^\infty\left[\frac{\beta^2 J_1(\hat{\rho}\beta)}{\hat{\rho}} - \beta^3 J_0(\hat{\rho}\beta)\right] \times \left\{\frac{\tilde{a}}{1+\beta\coth\beta}[-\hat{z}\cosh\hat{z}\beta + \coth\beta\sinh\beta\hat{z} + \beta(1-\hat{z})\sinh\beta\hat{z}] + \hat{b}(1-\hat{z})\sinh\beta\hat{z}\right\}d\beta - \frac{\cos\theta}{\sin\theta}\int_0^\infty \beta^2 J_1(\hat{\rho}\beta)\left\{\frac{\tilde{a}}{1+\beta\coth\beta}[\cosh\beta\hat{z}(1+\beta\coth\beta) + \beta^2(1-\hat{z})\sinh\beta\hat{z}] + \hat{b}[\sinh\beta\hat{z} + \beta(1-\hat{z})\cosh\beta\hat{z}]\right\}d\beta\right), \quad [61]$$

where differentiations appearing in [50]–[52] were carried out. Hence,

$$\left.\frac{\partial\omega_r}{\partial r}\right|_{r=0} = -\frac{2}{3}\frac{A}{H^3}\sin\theta\cos\phi\left[\left(\sin\theta\frac{\partial}{\partial\hat{\rho}} + \cos\theta\frac{\partial}{\partial\hat{z}}\right)(\quad)\right]_{\hat{\rho}=0,\hat{z}=\hat{h}}, \quad [62]$$

where the parentheses in [62] stand for the expression in parentheses in [61]. After some tedious arithmetic manipulations, we get

$$\left.\frac{\partial \omega_r}{\partial r}\right|_{r=0} = \frac{2}{3}\frac{A}{H^3}\sin\theta\cos\theta\cos\phi\left\{\int_0^\infty \frac{\beta^4}{\sinh^2\beta-\beta^2}[\hat{h}(k\sinh\beta-\beta t)\cosh(1-\hat{h})\beta + (1-\hat{h})(t\sinh\beta-k\beta)\cosh\hat{h}\beta]\,d\beta\right\}. \quad [63]$$

It is readily verified that [63] is symmetric with respect to $\hat{h}=\frac{1}{2}$ as expected. The integrand of [63] tends to $2\beta[3\hat{h}(1-\hat{h})+1]$ as $\beta\to 0$ and to $\beta^4\hat{h}^2\exp(-2\hat{h}\beta)$ as $\beta\to\infty$ and $\hat{h}\leqslant\frac{1}{2}$. Consequently, [63] converges and can easily be evaluated.

The total deformation of the droplet due to wall effects is obtained by summing the contributions of [58], [59] and [63] and introducing the total into [30]. Hence,

$$\delta_W = \frac{\mu a G}{\sigma}\left(\frac{a}{H}\right)^3\frac{\mu+2.5\mu'}{\mu+\mu'}\cdot\frac{16\mu+19\mu'}{8(\mu+\mu')}\cdot\sin\theta\cos\theta\cos\phi C_S, \quad [64]$$

where the shape factor C_S is

$$C_S = -\frac{1}{4}\sum_{m=1}^{\infty}\frac{1}{m^3}-\frac{1}{8}\sum_{m=0}^{\infty}\frac{1}{(m+\hat{h})^3}-\frac{1}{8}\sum_{m=1}^{\infty}\frac{1}{(m-\hat{h})^3}+\frac{2}{3}\int_0^\infty\frac{\beta^4}{\sinh^2\beta-\beta^2} \times[\hat{h}(k\sinh\beta-\beta t)\cosh(1-\hat{h})\beta+(1-\hat{h})(t\sinh\beta-k\beta)\cosh\hat{h}\beta]\,d\beta \quad [65]$$

and k and t are defined in [48a,b]. To obtain the total deformation, one has to add the Taylor deformation [31] to [65]. Equation [65] manifests that wall effects have not altered the shape of the deformed droplet, as predicted by Taylor. It has merely changed the magnitude of the deformation. For small ratios of a/h, [65] can be neglected altogether compared with [31]. However, as depicted in figure 2, if the droplet is close to the walls ($\hat{h}\to 0$ or $\hat{h}\to 1$), the shape coefficient C_S grows considerably. Notwithstanding, for droplets too close to the walls a three-reflection analysis might not be sufficient to describe the total hydrodynamic effect.

The asymptotic behavior of C_S for small $\hat{h}$ values is evaluated along the lines by which [55] was obtained (see appendix C). Hence, in the vicinity of the flat wall, we have

$$\lim_{h\to 0} C_S\cdot\hat{h}^3 = \tfrac{3}{8}, \quad [66]$$

which coincides with the result given by [32]. Chan & Leal (1979), who addressed a similar problem for a non-Newtonian fluid, obtained numerical values for C_S at three droplet locations $\hat{h}=0.2$, 0.3, 0.5, which exactly coincide with the results we present in table 2 (up to the first three significant digits).

6. CONCLUSIONS

The velocity and pressure fields around a droplet were calculated employing a reflection method. The method provided first-order approximations in a/h for the single-wall effect case and in a/H for the two-wall effect case. The drag force was affected by the walls via a term of order $(a/h)^2$ or $(a/H)^2$, respectively. The antisymmetric property of the drag coefficient proves that, for Couette

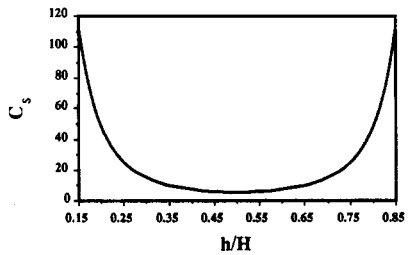

Figure 2. Shape factor [64] vs droplet position.

flows, a droplet located close to the wall at rest would lag behind the undisturbed velocity field, whereas a droplet located closed to the moving wall would move faster than the undisturbed velocity. A droplet located at the mid distance between the plates would move at a rate equal to the undisturbed velocity. (All aforementioned statements pertain to a location in the undisturbed field which coincides with the geometrical center of the droplet.) No transverse motion is observed for a spherical droplet although due to its deformation, a secondary transverse migration will occur. (Chaffey & Brenner 1967; Chaffey *et al.* 1965).

For the single- and two-wall effect cases a new mathematical method was applied in which integrations over a two-dimensional domain were replaced by integrations over a one-dimensional domain. It yielded explicit and rapidly converging expressions for the drag force and the deformation of the droplet. This simplicity made it possible to calculate and draw the numerical results over the whole domain of valid droplet locations. Ho & Leal (1974), who addressed a similar problem for rigid spheres, provide numerical values for four particle locations. Their results are obtained as a particular case for which $\mu' \to \infty$ (see table 1). Chan & Leal (1979), who addressed a similar problem for a non-Newtonian fluid, applied a different scheme of analysis which resulted in long two-dimensional integrals cited to exist in Chan's thesis. They provided numerical values for the shape factor at three droplet locations and for $a/H = 0.1$ and $\mu' = 0$, which coincide with our results exactly (see table 2). Their solution does not provide an explicit expression for the shape factor and drag coefficient dependence on μ'/μ. It is, however, implicitly given in their very complex integrals I_2 and I_5.

Table 1. The drag force factor

h/H	Two walls,[a] C_D	Single wall, $C_D = -1/8(H/h)^2$	Ho & Leal (1974) $(\mu' \to \infty)$
0.150	−0.53440262D + 01	−0.55555556D + 01	
0.175	−0.38521904D + 01	−0.40816327D + 01	
0.200	−0.28796228D + 01	−0.31250000D + 01	−2.8796
0.225	−0.22090946D + 01	−0.24691358D + 01	
0.250	−0.17259494D + 01	−0.20000000D + 01	−1.726
0.275	−0.13649326D + 01	−0.16528926D + 01	
0.300	−0.10866016D + 01	−0.13888889D + 01	−1.0868
0.325	−0.86589562D + 00	−0.11834320D + 01	
0.350	−0.68619014D + 00	−0.10204082D + 01	
0.375	−0.53601655D + 00	−0.88888889D + 00	
0.400	−0.40715838D + 00	−0.78125000D + 00	−0.4072
0.425	−0.29349386D + 00	−0.69204152D + 00	
0.450	−0.19025943D + 00	−0.61728395D + 00	
0.475	−0.93556601D − 01	−0.55401662D + 00	
0.500	0.00000000D + 00	−0.50000000D + 00	

[a] C_D is antisymmetric around $h/H = 0.5$.

Table 2. The shape factor

h/H	Two walls,[a] C_S	Single wall, $C_S = 3/8(H/h)^3$	Chan & Leal (1974) $(a/H = 0.1, \mu' = 0)$
0.125	0.19333713D + 03	0.19200000D + 03	
0.150	0.11233910D + 03	0.11111111D + 03	
0.175	0.71112829D + 02	0.69970845D + 02	
0.200	0.47955336D + 02	0.46875000D + 02	48.0
0.225	0.33963834D + 02	0.32921811D + 02	
0.250	0.25026798D + 02	0.24000000D + 02	
0.275	0.19066733D + 02	0.18031555D + 02	
0.300	0.14957296D + 02	0.13888888D + 02	15.0
0.325	0.12052477D + 02	0.10923987D + 02	
0.350	0.99646144D + 01	0.87463557D + 01	
0.375	0.84526356D + 01	0.71111111D + 01	
0.400	0.73626664D + 01	0.58593750D + 01	
0.425	0.65950786D + 01	0.48849990D + 01	
0.450	0.60856109D + 01	0.41152263D + 01	
0.475	0.57943842D + 01	0.34990523D + 01	
0.500	0.56996174D + 01	0.30000000D + 01	5.7

[a] C_S is symmetric around $h/H = 0.5$.

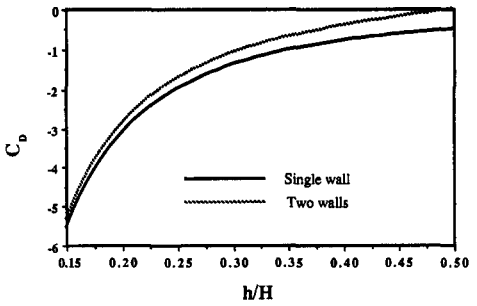

Figure 3. Comparison between single-wall and two-wall effects on the drag force coefficient for various droplet positions.

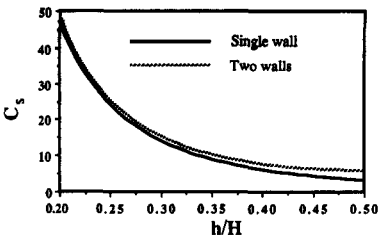

Figure 4. Comparison between single-wall and two-wall effects on the shape factor for various droplet positions.

A first-order wall effect was derived for the deformation of a droplet. It exhibits that the deformation shape derived by Taylor (1932, 1934) for a droplet suspended in an unbounded field is preserved, only the deformation magnitude has increased with a term of order $(a/H)^3$.

It is clear from figures 3 and 4 and from tables 1 and 2 that the so much simpler result derived for the single-wall effect may provide a very good approximation for h/H values as high as 0.25 with a 7% error for the drag coefficient and 2.5% error for the deformation coefficient.

Equations [28] and [54a,b] for the drag force and [32] or [64] for the deformation also manifest the effect of the flow circulation inside the droplet. For a rigid sphere case ($\mu' \Rightarrow \infty$) the drag force exerted on the particle is the largest. It is at most four times greater than that for a bubble ($\mu' \approx 0$), which is the least affected. Similarly, the wall effect on the droplet deformation is the largest for very viscous droplets. It is almost three times larger than the least affected bubble case. The rigid sphere case, however, (no deformation) cannot be recovered by taking ($\mu' \to \infty$) as explained by Taylor (1934) and Cox (1969).

It is interesting to note that, in our case, first-order wall effects on the drag force coefficient and droplet deformation are of the order of $(a/H)^2$ and $(a/H)^3$, respectively, whereas for the case of a droplet moving between two parallel walls in a quiescent fluid they are one order lower and thereby more pronounced (Shapira & Haber 1988).

Acknowledgement—This work is part of an M.Sc. Thesis submitted by M. Shapira to the Senate of the Technion and partially supported by the Deutsch Scholarship.

REFERENCES

ACRIVOS, A. & LO, T. S. 1978 Deformation and breakup of a single slender drop in an extensional flow. *J. Fluid Mech.* **86,** 641–672.

BARTHES-BIESEL, D. 1973 Deformation and burst of liquid droplets and non-Newtonian effects in dilute suspensions. Ph.D. Dissertation, Stanford Univ., Calif.

BARTOK, W. & MASON, S. G. 1959 Particle motion in sheared suspension, VIII. Singlets and doublets of fluid spheres. *J. Colloid Sci.* **14,** 13–26.

CHAFFEY, C. E. & BRENNER, H. 1967 A second-order theory for shear deformation of drops. *J. Colloid Interface Sci.* **24,** 258–269.

CHAFFEY, C. E., BRENNER, H. & MASON, S. G. 1965 Particle motions in sheared suspensions. *Rheol. Acta* **4,** 64–72.

CHAN, P. C. H. & LEAL, L. G. 1979 The motion of a deformable drop in a second-order fluid. *J. Fluid Mech.* **92,** 131–170.

COX, R. G. 1969 The deformation of a drop in a general time-dependent fluid flow. *J. Fluid Mech.* **37,** 601–623.

FRANKEL, N. A. & ACRIVOS, A. 1970 The constitutive equation for a dilute emulsion. *J. Fluid Mech.* **44,** 65–78.

GRACE, H. P. 1982 Dispersion phenomena in high viscosity immiscible fluid systems and application of static mixers as dispersion devices in such systems. *Chem. Engng Commun.* **14,** 225–277.

HABER, S. & ETSION, I. 1985 Analysis of an oscillatory oil squeeze film containing a central gas bubble. *ASLE Trans.* **28,** 253–260.

HABER, S., HETSRONI, G. & SOLAN, A. 1973 Low Reynolds number motion of two droplets. *Int. J. Multiphase Flow* **1,** 57–71.

HABER, S., SHAPIRA, M. & ETSION, I. 1987 The effect of two phase lubricant on bearing performance. *ASLE Trans.* **30,** 34–40.

HAPPEL, J. & BRENNER, H. 1965 *Low Reynolds Number Hydrodynamics.* Prentice-Hall, Englewood Cliffs, N.J.

HETSRONI, G. & HABER, S. 1970 The flow in and around a droplet or bubble submerged in an unbounded arbitrary velocity field. *Rheol. Acta* **9,** 488–498.

HETSRONI, G. & HABER, S. 1977 Low Reynolds number motion of two drops submerged in an unbounded arbitrary velocity field. *Int. J. Multiphase Flow* **4,** 1–17.

HIBNER, D. H. & BANSEL, P. N. 1979 Effects of fluid compressibility on viscous damper characteristics. Presented at a *Wkshp on Solubility and Dynamic Response of Rotors with Squeeze Film Bearings*, Charlottesville, Va.

HINCH, E. J. & ACRIVOS, A. 1980 Long slender drops in simple shear flow. *J. Fluid Mech.* **98,** 305–328.

HO, B. P. & LEAL, L. G. 1974 Inertial migration of rigid spheres in two dimensional unidirectional flows. *J. Fluid Mech.* **65,** 365–400.

LIRON, N. & MOCHON, S. 1976 Stokes flow for a stokeslet between two parallel flat plates. *J. Engng Math.* **10,** 287–303.

MARSH, H. 1974 Cavitation in dynamically loaded journal bearings. In *Proc. 1st Leeds–Lyon Symp. on Tribology*, pp. 91–95.

PARKINS, D. W. & STANLEY, W. T. 1982 Characteristics of an oil squeeze film. *Trans. ASME J. Lubric. Technol.* **104,** 497–503.

RUMSCHEIDT, F. D. & MASON, S. G. 1961a Particle motion in sheared suspension, XI. Internal circulation in fluid droplets (experimental). *J. Colloid Sci.* **16,** 210–237.

RUMSCHEIDT, F. D. & MASON, S. G. 1961b Particle motion in sheared suspension, XII. Deformation and burst of fluid drops in shear and hyperbolic flow. *J. Colloid Sci.* **16,** 238–261.

SHAPIRA, M. & HABER, S. 1988 Low Reynolds number motion of a droplet between two parallel flat plates. *Int. J. Multiphase Flow* **14,** 483–506.

SNEDDON, I. N. 1951 *Fourier Transforms.* McGraw-Hill, New York.

TAYLOR, G. I. 1932 The viscosity of a fluid containing small drops of another fluid. *Proc. R. Soc. Lond.* **A138,** 41–48.

TAYLOR, G. I. 1934 The formation of emulsions in definable fields of flows. *Proc. R. Soc. Lond.* **A146,** 501–523.

TORZA, S., COX, R. G. & MASON, S. G. 1972 Particle motion in sheared suspension, XXVII. Transient and steady deformation and burst of liquid drops. *J. Colloid Interface Sci.* **38,** 395–411.

WHITE, D. C. 1970 Squeeze film journal bearings. Ph.D. Dissertation, Cambridge Univ., U.K.

APPENDIX A

A general solution for Stokes equations in cartesian coordinates x, y, z, when x, y are unbounded, can be derived using a two-dimensional Fourier transform

$$\tilde{p}(\lambda_1, \lambda_2, z) = \frac{1}{2\pi} \int\int_{-\infty}^{\infty} p(x, y, z) \exp[i(\lambda_1 x + \lambda_2 y)] \, dx \, dy, \qquad [A.1]$$

where $p(x, y, z)$ is a fucntion in real space and $\tilde{p}(\lambda_1, \lambda_2, z)$ is its Fourier transform. The inverse transform is

$$p(x, y, z) = \int\int_{-\infty}^{\infty} \tilde{p}(\lambda_1, \lambda_2, z) \exp[-i(\lambda_1 x + \lambda_2 y)] \, d\lambda_1 \, d\lambda_2. \qquad [A.2]$$

Applying Fourier's transform on Stokes equations, one obtains, after some simple manipulations, that $\tilde{\omega}_z$, the transformed z component of the velocity field, satisfies the following fourth-order ordinary linear differential equation:

$$\left[\frac{d^2}{dz^2} - (\lambda_1^2 + \lambda_2^2)\right]^2 \tilde{\omega}_z = 0. \tag{A.3}$$

A general solution of [A.3] can easily be derived:

$$\tilde{\omega}_z = (\tilde{A}_1 + \tilde{A}_2 z)\cosh \lambda z + (\tilde{A}_3 + \tilde{A}_4 z)\sinh \lambda z, \tag{A.4}$$

where

$$\lambda = \{\lambda_1^2 + \lambda_2^2\}^{1/2}$$

and the coefficients $\tilde{A}_i$ $(i = 1, \ldots, 4)$ are general functions of λ_1 and λ_2. If one deals with a semi-infinite domain $z \geqslant 0$, e.g. the case analyzed in section 2, the velocity field must vanish at $z \to \infty$ and [A.4] assumes the form

$$\tilde{\omega}_z = \tilde{C} \exp(-\lambda z) + \tilde{D} z \exp(-\lambda z), \tag{A.5}$$

which depends only on two coefficients, $\tilde{C}$ and $\tilde{D}$. The other transformed velocity components $\tilde{\omega}_x$ and $\tilde{\omega}_y$ and the pressure fields $\tilde{s}$ are

$$\tilde{\omega}_x = \left(\tilde{A} + \frac{i\lambda_1}{\lambda} z\tilde{D}\right)\exp(-\lambda z), \tag{A.6a}$$

$$\tilde{\omega}_y = \left(\tilde{B} + \frac{i\lambda_2}{\lambda} z\tilde{D}\right)\exp(-\lambda z) \tag{A.6b}$$

and

$$\tilde{s} = 2\tilde{D} \exp(-\lambda z), \tag{A.6c}$$

where two additional yet undetermined coefficients $\tilde{A}$ and $\tilde{B}$ are introduced. Satisfaction of the continuity equation requires that

$$\tilde{D} = \lambda\tilde{C} + i(\lambda_1 \tilde{A} + \lambda_2 \tilde{B}). \tag{A.7}$$

Hence only three coefficients out of four are independent and can be determined via the three boundary conditions imposed on the velocity field at $z = 0$.

In our case (section 2), since $\omega_x = \omega_y = 0$ at $z = 0$ see [23b,c], it implies that

$$\tilde{A} = \tilde{B} = 0, \quad \tilde{D} = \lambda\tilde{C}. \tag{A.8}$$

From [23a] we have that

$$\omega_z\big|_{z=0} = \frac{2Ah^2x}{(h^2 + \rho^2)^{5/2}}, \tag{A.9}$$

where $\rho^2 = x^2 + y^2$.

However, from the Lipschitz integral we have that

$$\frac{1}{(\rho^2 + h^2)^{1/2}} = \int_0^\infty J_0(\rho\lambda)\exp(-\lambda|h|)\, d\lambda. \tag{A.10}$$

Differentiating [A.10] consecutively with respect to h and x, we get

$$\frac{2Ah^2x}{(\rho^2 + h^2)^{5/2}} = -\tfrac{2}{3}A|h|\frac{\partial}{\partial x}\int_0^\infty J_0(\rho\lambda)\exp(-\lambda|h|)\lambda\, d\lambda. \tag{A.11}$$

However, Sneddon (1951) has shown that the two-dimensional Fourier transform is equal to the zero-order Hankel transform if a function $P(\lambda_1, \lambda_2)$ can be expressed in terms of λ only, namely:

$$\frac{1}{2\pi}\int\int_{-\infty}^{\infty} P(\lambda)\exp[-i(\lambda_1 x + \lambda_2 y)]\, d\lambda_1\, d\lambda_2 = \int_0^\infty \lambda J_0(\lambda\rho)P(\lambda)\, d\lambda. \tag{A.12}$$

Hence [A.11] can be rewritten as

$$\frac{2Ah^2x}{(\rho^2+h^2)^{5/2}}=\frac{1}{3\pi}A|h|i\int\int_{-\infty}^{\infty}\lambda_1\exp(-\lambda|h|)\exp[-i(\lambda_1x+\lambda_2y)]\,dx\,dy$$

or

$$\tilde{\omega}_z|_{z=0}=\frac{i\lambda_1}{3\pi}Ah\exp(-\lambda h). \tag{A.13}$$

Introducing [A.13] into [A.5] we obtain

$$\tilde{C}=\frac{Ah}{3\pi}i\lambda_1\exp(-\lambda h). \tag{A.14}$$

Consequently, from [A.2], [A.5], [A.8] and [A.14], the solution for ω_z is

$$\begin{aligned}\omega_z&=\frac{Ah}{3\pi}i\int\int_{-\infty}^{\infty}\lambda_1\exp[-\lambda(h+z)](1+\lambda z)\exp[-i(\lambda_1x+\lambda_2y)]\,d\lambda_1\,d\lambda_2\\&=-\tfrac{2}{3}Ah\frac{\partial}{\partial x}\int_0^{\infty}\exp[-\lambda(h+z)](1+\lambda z)J_0(\lambda\rho)\,d\lambda.\end{aligned} \tag{A.15}$$

If we replace h by $h+z$ in [A.10] and use its derivatives with respect to $h+z$, the last integral is simply

$$\omega_z=\frac{2Ahx}{r_2^7}[hr_2^2+5z(h+z)^2], \tag{A.16}$$

where $r_2=[(h+z)^2+\rho^2]^{1/2}$. The velocity components ω_x and ω_y and the pressure s are found similarly and [24] and [25] are recovered.

APPENDIX B

Equation [39a] is transformed using [A.11], namely

$$\left[2Ax\frac{(h+2mH)^2}{r_m^5}\right]_{z=0}=-\frac{2A}{3}|h+2mH|\frac{\partial}{\partial x}\int_0^{\infty}J_0(\lambda\rho)\exp(-\lambda|h+2mH|)\lambda\,d\lambda. \tag{B.1}$$

Hence, from [A.12] and [39a],

$$\tilde{\omega}_z|_{z=0}=\frac{i\lambda_1A}{3\pi}\sum_{m=-\infty}^{\infty}|h+2mH|\exp(-\lambda|h+2mH|) \tag{B.2}$$

$$=-\frac{i\lambda_1A}{3\pi}\frac{\partial}{\partial\lambda}\sum_{m=-\infty}^{\infty}\exp(-\lambda|h+2mH|). \tag{B.3}$$

However, the sum in [B.3] can be decomposed into three terms

$$\sum_{m=-\infty}^{\infty}\exp(-\lambda|h+2mH|)=\exp(-\lambda h)+\sum_{m=1}^{\infty}\exp[-\lambda(h+2mH)]+\sum_{m=1}^{\infty}\exp[-\lambda(2mH-h)], \tag{B.4}$$

where the last two are simple geometric series. Consequently, after some simple arithmetic manipulations,

$$\tilde{\omega}_z|_{z=0}=-\frac{i\lambda_1A}{3\pi}\frac{\partial}{\partial\lambda}\left(\frac{\cosh\lambda(H-h)}{\sinh\lambda H}\right). \tag{B.5}$$

Similarly, the transformed boundary condition [39b] is

$$\tilde{\omega}_z|_{z=H}=-\frac{i\lambda_1A}{3\pi}\frac{\partial}{\partial\lambda}\left(\frac{\cosh\lambda h}{\sinh\lambda H}\right). \tag{B.6}$$

Utilizing [44], [49] and [39a,b], [46]–[48] are recovered.

APPENDIX C

The asymptotic behavior of C_D for $\hat{h} \to 0$ needs some careful evaluation since the integration domain extends to infinity and products of $\hat{h}\beta$ exist in the following integral:

$$C_D = \int_0^\infty f(\hat{h}, \beta)\, d\beta, \qquad [C.1]$$

where $f(\hat{h}, \beta)$ is given by [54b]. To circumvent this difficulty we divide the integration domain into two parts

$$C_D = \int_0^N f(\hat{h}, \beta)\, d\beta + \frac{1}{\hat{h}} \int_{N\hat{h}}^\infty f(\hat{h}, x)\, dx, \qquad [C.2]$$

where $N = O(\hat{h}^{-q})$, for $0 < q < 1$, spans an intermediate range. Consequently, for the first integral $f(\hat{h}, \beta)$ can be expanded in terms of $\hat{h}$ for β fixed. In the second integral we expand $f(\hat{h}, x)$ in terms of $\hat{h}$ for $x = \beta\hat{h}$ fixed.

The first integrand results in the following expansion of [54b]:

$$\hat{h} \int_0^N \frac{1}{3} \frac{\beta^4(\cosh\beta - 1)}{\sinh^2\beta(\sinh\beta - \beta)}\, d\beta + O(\hat{h}^2), \qquad [C.3]$$

which decays regularly like $\hat{h}$ (the integral is finite independent of N to the extent of terms exponentially small).

The leading term of the second integral is

$$-\frac{1}{3\hat{h}^2} \int_{\hat{h}N}^\infty x^3 \exp(-2x)\, dx \xrightarrow{\hat{h}\to 0} -\frac{1}{8\hat{h}^2}. \qquad [C.4]$$

Thus, the singular term stems from the second integral only, and

$$\lim_{\hat{h}\to 0} C_D \to -\frac{1}{8\hat{h}^2}.$$

The deformation coefficient C_S given in [65] can be treated similarly. The second term in [65] contributes $-1/8h^3$ and the integral term contributes

$$\frac{2}{3\hat{h}^3} \int_{N\hat{h}}^\infty x^4 \exp(-2x)\, dx \xrightarrow{\hat{h}\to 0} \frac{1}{2\hat{h}^3}.$$

Thus, we have

$$\lim_{\hat{h}\to 0} C_S \to \frac{3}{8\hat{h}^3}.$$